Wright, Amanda J. and Richens, Joanna L. and Bramble, J.P. and Cathcart, N. and Kitaev, V. and O'Shea, Paul and Hudson, A.J. (2016) Surface-enhanced Raman scattering measurement from a lipid bilayer encapsulating a single decahedral nanoparticle mediated by an optical trap. Nanoscale, 8 (36). pp. 16395-16404. ISSN 2040-3364

Nanoscale

PAPER

View Article Online
View Journal | View Issue

Cite this: *Nanoscale*, 2016, **8**, 16395

Surface-enhanced Raman scattering measurement from a lipid bilayer encapsulating a single decahedral nanoparticle mediated by an optical trap

A. J. Wright,*†[a] J. L. Richens,[b] J. P. Bramble,[b] N. Cathcart,[c] V. Kitaev,[c] P. O'Shea[b] and A. J. Hudson†[d]

Received 15th July 2016,
Accepted 30th August 2016

DOI: 10.1039/c6nr05616d

www.rsc.org/nanoscale

We present a new technique for the study of model membranes on the length-scale of a single nano-sized liposome. Silver decahedral nanoparticles have been encapsulated by a model unilamellar lipid bilayer creating nano-sized lipid vesicles. The metal core has two roles (i) increasing the polarizability of vesicles, enabling a single vesicle to be isolated and confined in an optical trap, and (ii) enhancing Raman scattering from the bilayer, *via* the high surface-plasmon field at the sharp vertices of the decahedral particles. Combined this has allowed us to measure a Raman fingerprint from a single vesicle of 50 nm-diameter, containing just ~10^4 lipid molecules in a bilayer membrane over a surface area of <0.01 μm^2, equivalent to a volume of approximately 1 zepto-litre. Raman scattering is a weak and inefficient process and previous studies have required either a substantially larger bilayer area in order to obtain a detectable signal, or the tagging of lipid molecules with a chromophore to provide an indirect probe of the bilayer. Our approach is fully label-free and bio-compatible and, in the future, it will enable much more localized studies of the heterogeneous structure of lipid bilayers and of membrane-bound components than is currently possible.

Introduction

Lipid vesicles (liposomes) are a common model cell system used to investigate membrane processes such as lipid–protein interactions. Despite the ability to prepare suspensions of lipid vesicles by high pressure extrusion techniques[1] with a unilamellar bilayer structure, a fixed diameter (40–100 nm; 1 zepto-litre volume) and low polydispersity index (~0.1), the molecular composition and structure of the lipid bilayer is inherently heterogeneous. For instance, the different lipid molecules in a multicomponent mixture will be distributed non-uniformly and this can result in the appearance of phase-separated microdomains in bilayer regions across an ensemble of vesicles. A single vesicle of 50 nm diameter assembled from only ~1.6×10^4 lipid molecules in a unilamellar membrane over a surface area of <0.01 μm^2 (assuming an outer leaflet radius of 25 nm, inner leaflet radius of 21 nm and a lipid area of 0.82 nm^2; see (2)), will be highly sensitive to local features (such as micro-domains) and the presence of small numbers of guest molecules (such as proteins). Therefore, there is a need to develop a methodology to interrogate these model cell systems at the single vesicle level in order to detect both changes in membrane structure and properties, and to understand how the extent of these changes might vary across the ensemble of vesicles. This has not previously been possible.

We present a novel measurement technique that allows the composition of ~1.6×10^4 lipid molecules in a single 50 nm diameter lipid vesicle to be monitored. We combined optical trapping with Raman spectroscopy to isolate individual vesicles and detected their Raman scattering signatures. The lipid vesicles themselves have been designed to encapsulate single silver decahedral nanoparticles enhancing the Raman scattering from the lipid bilayer *via* a surface-plasmon effect and increasing the polarizability of the vesicles allowing them to be optically trapped. An overview of this new approach can be seen in the schematic presented in Fig. 1 showing the two overlapping laser beams and the lipid encapsulated metal nanoparticle.

Developing optical techniques with sufficient sensitivity to monitor changes in membrane composition of a single vesicle,

[a]*Department of Electrical and Electronic Engineering, University of Nottingham, Nottingham, NG7 2RD, UK. E-mail: amanda.wright@nottingham.ac.uk*
[b]*Faculty of Pharmaceutical Sciences, 2405 Wesbrook Mall, Vancouver, BC Canada, V6T 1Z3*
[c]*Department of Chemistry and Biochemistry, Wilfrid Laurier University, Waterloo, ON, N2L 3C5, Canada*
[d]*Department of Chemistry, University of Leicester, Leicester, LE1 7RH, UK*
† These authors contributed equally to this work.

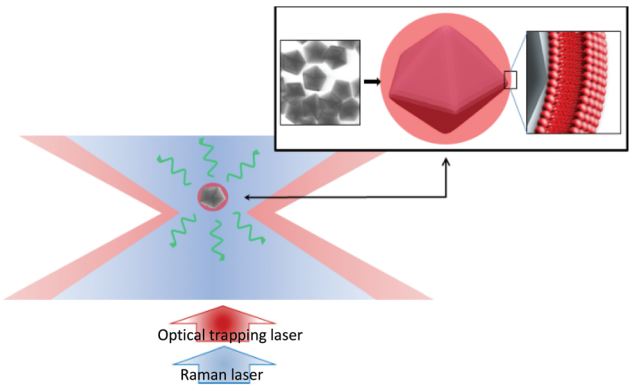

Fig. 1 A schematic diagram showing two spatially overlapping laser beams, red the optical trapping beam and blue the Raman excitation beam. At the focus of the two beams a liposome encapsulated decahedral nanoparticle is isolated and confined to the focal volume of the optical trapping beam and the light from the Raman excitation laser is scattered to generate the Raman signature of the lipid molecules (depicted as green photons). The insert represents the encapsulated decahedral nanoparticle showing a transmission electron microscopy micrograph of decahedral nanoparticles and the minimal gap between the metal and the lipid bilayer.

when such few molecules are present, is challenging. Raman spectroscopy has the ability to produce a characteristic fingerprint related to both the specific vibrational modes and environment of molecules present in a sample, and would in many ways be the ideal approach for monitoring time-dependent changes in membrane composition and structure.[3–5] Previous studies that have recorded the Raman spectra from lipid molecules have either illuminated an 80 × 40 μm area on a lipid bilayer containing approximately 8×10^9 lipid molecules[3] or optically trapped a large unilamellar vesicle approximately 1 μm in diameter with roughly 3×10^7 lipid molecules.[4,5] Unfortunately, Raman scattering cross-sections are low (typically 8–10 orders of magnitude lower than fluorescence[6]), prohibiting measurement of a small number of molecules in the absence of any enhancement mechanism. In 2011, Ip *et al.* demonstrated enhanced Raman scattering from an ensemble of spherical gold nanoparticles encapsulated by a lipid bilayer, with a nanoparticle diameter of 60 nm and overall vesicle diameter of <100 nm, in this earlier work, the Raman signatures recorded were that of a chromophore (for example, malachite green isothiocyanate) conjugated to lipid molecules in the bilayer structure.[7] More recently, Bhowmik *et al.* have studied Amyloid-β attachment to lipid coated spherical nanoparticles using label-free enhanced Raman scattering approach measuring bulk signal from a collection of vesicles.[8]

For surface enhanced Raman scattering (SERS), the molecule or sample of interest has to be in close proximity to a roughened metal surface and the frequency of the laser radiation selected to excite a surface plasmon in the metal, which creates 'hot-spots' of localized and enhanced optical field to give a greatly increased scattering signal.[9,10] In the work reported by Ip *et al.*,[7] the chromophore provides an additional enhancement mechanism derived from complementarity between the surface plasmon frequency and an excited-electronic state in the molecule of interest; the resulting scattering signal being enhanced by the plasmon resonance as well as the electronic resonance of the chromophore. This photophysical process is termed surface-enhanced resonant Raman scattering (SERRS). Impressive enhancement factors of the order of 10^6 in SERS and 10^{13}–10^{15} in SERRS have been reported in the literature.[9]

For SERS/SERRS, the structure of the metal surface is important as roughness or nanoscale features are necessary to create local 'hot-spots' in the surface plasmon-polariton wave. In this case, the field is no longer confined to the surface of the metal object but instead is able to couple to the local environment. Svedberg *et al.* isolated single spherical gold nanoparticles, coated with thiophenol, in an optical trap and demonstrated that Raman scattering was below the detection limit.[11] The authors showed that it was critical to bring a pair of spherical nanoparticles into close contact using optical tweezers to measure a SERS spectrum from surface-bound thiophenol.[11] Xu *et al.* modelled the influence of particle shape, size and composition on the electromagnetic contributions to SERS showing that the maximum enhancement factor is only achievable at sites between particles or at sharp protrusions on the surface.[10]

The metal nanoparticles used in this study were selected to maximize the SERS enhancement making the Raman scattering signal from the lipid molecules detectable. The SERS enhancement process is a near-field plasmonic effect that falls off rapidly with distance from the metal surface to the molecule of interest, the size of the nanoparticles were selected to produce a snug-fit between the lipid bilayer and nanoparticle and to minimise any gap. Decahedral shaped nanoparticles were selected due to their sharp vertices and edges which are essential features of all SERS experiments. Decahedral nanoparticles have been shown to produce superior SERS enhancements compared to cubes and octahedra.[12] Standridge *et al.* have shown that the enhancement range is operational at least within 10 nm from the tip/edge.[13] Therefore, for decahedral nanoparticles ~40 nm in diameter (sides <25 nm) the majority of the vesicles will be within 10 nm of vertices and edges ensuring successful reporting from the entire bilayer surface coating of the particle not just the local regions of bilayer near tips/edges. 40–45 nm diameter silver decahedral nanoparticles have a resonance peak between 470–480 nm close to the 488 nm wavelength of our Raman excitation beam.

To isolate individual liposomes and record the Raman signal from lipid molecules, we use an apparatus that combines optical trapping with Raman microspectroscopy, where an optical trap is created by a near-infrared laser focused to a diffraction-limited beam waist and Raman excitation is facilitated by a visible laser which is also focused to a diffraction-limited beam waist. In practice this means that the pico-Newton level forces from the trapping laser pulls the liposomes into the focal volume of the Raman laser, where an individual liposome is held transiently to enable the Raman signal to be measured. Without the optical-trapping system, it

is impossible to locate and characterize vesicles with sizes below the diffraction limit of the microscope. The combination of optical trapping and Raman spectroscopy is a very powerful technique for reversibly immobilizing particles in a sample and simultaneously characterizing their chemical composition.[14] To date, the majority of applications of Raman tweezers have involved the measurement of micron-sized particles, in excess of 1 femtolite volume, where the target molecules are distributed throughout the entire volume;[14] in many cases, the Raman signal has still been enhanced by electronic resonance or optical cavity conditions.[15]

In this paper we show that a single decahedral nanoparticle can create local electric-field 'hot-spots' and enhance the Raman scattering from probe thiophenol molecules present on the particle surface; the results will be contrasted to the weak enhancement provided by a single spherical nanoparticle. Using a Raman tweezers system we then demonstrate that an enhanced lipid Raman signal can be observed from a single, optically trapped, membrane-encapsulated decahedral nanoparticle approximately 1 zl in volume (50 nm in diameter). We compare the frequency of SERS events recorded in suspensions of both decahedral and spherical nanoparticles encapsulated by a lipid membrane, and discuss the importance of nanoparticle size and shape on enhancing Raman scattering from lipids in bilayers of low surface area.

We have supported the data demonstrating SERS activity of membrane-encapsulated decahedral nanoparticles with evidence that the enhancement is achieved from single isolated vesicles. To confirm single nanoparticle encapsulation and the absence of aggregation in our samples, we present transmission electron micrographs that illustrate the presence of single decahedral nanoparticles within a lipid bilayer shell and dynamic light scattering data that demonstrates the absence of any detectable aggregation of lipid-coated nanoparticles subsequent to encapsulation in a lipid bilayer. Control experiments, utilizing membrane-encapsulated spherical nanoparticles, and low concentration samples, eliminate the possibility that the signal was being measured from multiple (*i.e.* aggregated) vesicles in the optical trap.

This novel approach combining optical trapping with Raman spectroscopy to study individual 50 nm dimeter lipid vesicles containing a metal nanoparticle core, represents an increase in sensitivity of between 100 to 100 000 compared to current state-of-the-art label free measurements techniques.[3–5] In future this will enable highly-sensitive Raman approaches to be used to the study the of interactions of guest molecules with lipids at the low number of molecule level. Importantly, our approach isolates a single vesicle from the ensemble for spectroscopic investigation and is label-free.

Methods

Optical system

The Raman tweezers system is based on an inverted microscope using a continuous wave near-infra red (NIR) laser as the optical trapping beam (λ = 1070 nm) and a continuous wave narrow line width visible laser as the Raman excitation beam (λ = 488 nm) in a similar arrangement to that presented in Petrov 2007.[14] A dichroic mirror was used to combine the two beams ahead of the back aperture of an objective lens with a high numerical aperture (N.A. = 1.25) to provide the intensity gradient required for optical trapping and a diffraction–limited beam waist for confocal Raman microscopy. A spatial light modulator was placed in the path of the optical-trapping laser and used for fine adjustments of the trap position, which ensured that the particle was located in the waist of the Raman laser. Accounting for losses from the spatial light modulator, dichroic mirror and objective lens, a NIR-laser power of 90 mW and a visible-laser power of 5 mW was estimated in the sample plane. The sample plane was viewed in transmission using a white light LED source and a monochrome CCD camera. Inelastic light scattered from the focal volume of the Raman laser was imaged onto a confocal pinhole ahead of the spectrograph to reduce background. The spatially-filtered light was re-imaged using a 50 mm achromatic lens onto the 100 μm-width entrance slits of the spectrograph (0.500 m focal length triple grating, 600 lines per mm, 500 nm blaze wavelength; Acton Research Corporation, Spectra Pro 2500i). The detector used was a −80 °C cooled back-illuminated, charge-coupled device (Princeton Instruments, Pixis 100B).

Sample preparation – thiophenol coated nanoparticles

Decahedral silver nanoparticles, purchased from Sciventions (Toronto, Canada) at a concentration of 0.1 mM, with sizes ranging from 36 to 44 nm, were prepared according to procedures described previously with poly (sodium 4-styrene sulfonate) substituted for poly vinyl pyrrolidone.[16] Pietrobon *et al.* showed that the absorbance maximum for these decahedral nanoparticles occurred in the wavelength range of 450 nm to 470 nm depending on the particle size.[16] The absorption spectra of the decahedral nanoparticles have been recorded after 6 months of storage and show no signs of oxidation and aggregation. Spherical silver nanoparticles of 40 nm in diameter were purchased from BBI Solutions (Cardiff, UK) at a concentration of 0.03 mM and measured in-house to have an absorbance maximum at a wavelength of 405 nm. The decahedral nanoparticles have a citrate (*ca.* 2 mM in a native solution) and poly(sodium 4-styrenesulfonate), PSS, (*ca.* 0.05 mM in native solution) coating and the spherical nanoparticles have a citrate coating. The coatings act as a charge stabilizer and prevent aggregation. Raman spectra of optically trapped nanoparticles without thiophenol or lipid membrane show only an elastic-scattering signal (measured on a CCD camera) and a background Raman signal from the buffer solution and with no peaks present due to the PSS or citrate. 1 part of the nanoparticle suspensions was diluted in 2 parts of 10 mM Tris pH 7.4. A few drops of a solution of thiophenol in ethanol (approx. 1 mM) were added to the suspensions. The final concentration of thiophenol exceeded monolayer coverage of the nanoparticles.

Sample preparation – membrane vesicles with and without nanoparticles

The preparation of membrane vesicles in the presence and absence of silver nanoparticles (which were not coated with thiophenol) was based upon procedures described previously.[17,18] Briefly, phosphatidylcholine (PC) was dissolved in chloroform in a round bottom flask and dried under a stream of oxygen-free nitrogen gas until a thin film was formed. The lipid film was rehydrated with the appropriate buffer (to 3.25 mM), either in the presence or absence of silver nanoparticles (either spherical or decahedral). The resulting multilamellar solution was frozen and thawed 10 times. Suspensions were introduced into an extruder (Lipex Biomembranes Inc., Vancouver, Canada) and passed 10 times through 25 mm diameter polycarbonate filters with pores of 50 nm in diameter (Nuclepore Filtration Products, Whatman, Piscataway, NJ); to ensure single nanoparticle encapsulation and size uniformity, according to previously described procedures.[17] This resulted in a monodisperse, unilamellar suspension of phospholipid vesicles or phospholipid-encapsulated nanoparticles. The composition of a representative batch of the egg phosphatidylcholine (from Lipid Products UK) is 32.1% 16:0 (DPPC), 2.1% 16:1 Δ9 (*cis*/*trans*), 11.7% 18:0 (DSPC), 36.2% 18:1 (DOPC), 12.5% 18:2 (DLPC) and 5.5% 20:4 PC.

The initial concentration of lipid (3.25 mM) was kept constant across the range of samples made and the same dilution of 1 part of the nanoparticle suspension to 2 parts of 10 mM Tris pH 7.4 were used. The final concentration of vesicles is assumed to be the same across all the samples made and the vesicles, with either a nanoparticle or an aqueous core, were used within 24 hours of sample preparation. Any excess nanoparticles that had not been encapsulated did not pass through the polycarbonate filter. A metal deposit was clearly visible on the filter at the end of the process and, therefore, non-encapsulated nanoparticles were not present in the final sample. Extrusion through a pore size of 50 nm diameter in the presence of nanoparticles ranging in size from 36–44 nm ensured that only a thin aqueous layer of <6 nm thickness will remain between the inner leaflet of the lipid membrane and the metal particle. The expected thickness of a lipid bilayer is 4.0 ± 0.5 nm.[2,19]

Sample preparation – giant unilamellar vesicles (GUVs)

Giant unilamellar vesicles (GUV) were made as a control measurement of the lipid-Raman spectrum for a unilamellar membrane. They were produced using a rapid evaporation technique to give a population of vesicles ranging in size from 2–50 μm.[20]

Transmission electron microscope (TEM)

The lipid encapsulated decahedral nanoparticles were imaged on a FEI Tecnai transmission electron microscope (TEM). To prepare a sample for imaging, 13 μl of the membrane encapsulated decahedral nanoparticle suspension was dropcast onto a 200 mesh carbon-coated copper TEM grid (Agar Scientific, UK). After 5 minutes the solution was blotted away. To visualize the lipid coating, the grids were then negatively stained with 3% Uranyl Acetate solution, the lipid film itself does not stain and appears bright against the dark background. 5 μl of staining solution was loaded on to the grid, after 30 seconds the grid was blotted to remove excess solution.

Results

The optical trapping power was selected to pull individual nanometer-sized vesicles into the beam waist and temporarily restrict their Brownian motion whilst the Raman scattering signal was recorded (see schematic overview in Fig. 1). For each experiment, the spectrograph was set to record spectra with either a 1 or 2 second acquisition time over a 30 minute time period (resulting in 1800 or 900 individual spectra respectively). A LabVIEW program was developed to analyze each set of spectra by subtracting the background signal level and plotting the peak height against time for either the overlapping C–H bands at c. 2900 cm^{-1} from lipid or the C–C band at c. 1600 cm^{-1} from thiophenol. The resulting plots illustrated short bursts in signal intensity corresponding to SERS events. The number of SERS events in a time window of 30 minutes was determined and the different samples compared quantitatively. This technique proved to be an effective means to determine the SERS activity of a nanoparticle sample.

Encapsulation of single decahedral nanoparticles in a lipid bilayer

To demonstrate successful encapsulation of the decahedral nanoparticles in a lipid bilayer the samples were imaged using a transmission electron microscope (TEM), see Method section for further details. Fig. 2 compares TEM images of a lipid membrane-encapsulated decahedral nanoparticle and a decahedral nanoparticle without the lipid membrane, the bilayer of lipid molecules surrounding the nanoparticle can be clearly identified along the faces of the nanoparticle in Fig. 2b). The

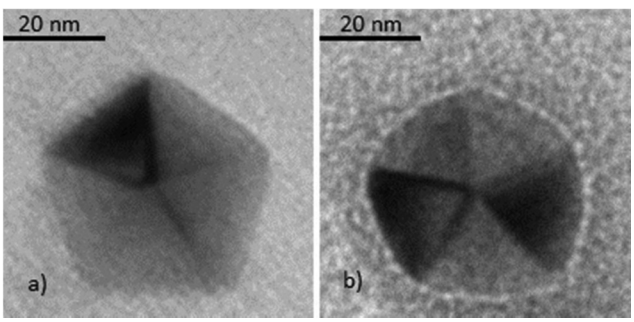

Fig. 2 Transmission electron microscopy (TEM) images of (a) a 41 nm diameter silver decahedral nanoparticle and (b) a membrane-encapsulated 41 nm diameter decahedral nanoparticle. The TEM grids for (a) and (b) were negatively stained with 3% uranyl acetate solution to improve the contrast of the lipid bilayer surrounding the nanoparticles in image (b) and as a control in image (a).

samples have been negatively stained to increase the contrast around the particle. The lipid film itself does not stain and appears as a thick bright line surrounding the nanoparticles.

For each sample the particle size and monodispersity of the sample preparation was confirmed using dynamic-light scattering (Malvern, ZetaSizer NS). For the five membrane-encapsulated nanoparticle samples examined, the particle diameter at the peak maximum in the number density distribution ranged from 42–51 nm and the polydispersity index ranged from 0.06–0.17. As a guide a polydispersity index >0.7 would mean that the sample was polydisperse, a polydispersity index below 0.2 (as measured here) implies a highly monodisperse sample. Hence, the dynamic-light scattering results combined with the TEM images provide clear evidence that the samples contained individual vesicles in suspension without aggregation.

Impact of nanoparticle shape on SERS enhancement

Initially decahedral and spherical nanoparticles were coated with a thiophenol monolayer to understand the impact of nanoparticle shape on the Raman scattering cross-section. The monolayer coating of thiophenol provides a useful probe and any SERS-scattered light from the thiophenol molecules was detected and used to determine how effective a particular nanoparticle shape was at enhancing the Raman-scattered light. A similar thiolophenol monolayer was used by Svedberg *et al.*[11] when comparing SERS from single spherical nanoparticles to pairs of spherical nanoparticles. Fig. 3 shows an example of a thiophenol SERS spectrum from an optically-trapped decahedral silver nanoparticle recorded over an integration time of 2 seconds. The main peak at 1586 cm^{-1} corresponds to the C–C symmetric-stretching mode of the thiophenol molecules. The positions of the peaks in Fig. 3 are in agreement with the thiophenol spectra presented in Svedberg *et al.*[11] It should be noted that a series of spectra were recorded of just the decahedral nanoparticles as a control, the only features present were those of the background buffer solution.

Fig. 4 compares the bursts of Raman-scattered light recorded from 36 nm diameter silver decahedral nanoparticles and 40 nm diameter silver spherical nanoparticles coated with a monolayer of thiophenol. Here, 2 second spectra were recorded over at total time period of 30 minutes whilst the trapping beam guided the nanoparticles into the focal volume of the Raman excitation laser. The nanoparticles were confined for only a few seconds before exiting the optical trap. In Fig. 4 the height of the C–C symmetric-stretching mode in the thiophenol Raman spectrum is plotted as a function of time showing distinct Raman bursts where a nanoparticle has been confined by the optical trap and the metal surface from the nanoparticle has enhanced the Raman scattering signal from the adsorbed thiophenol.

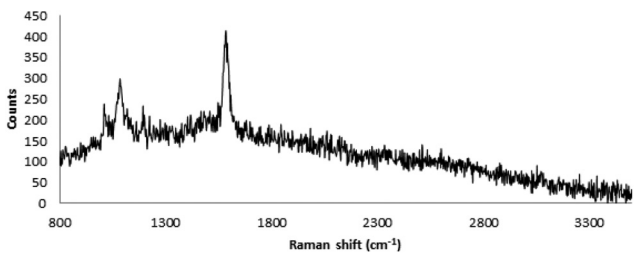

Fig. 3 A SERS spectrum recorded from an optically-trapped 36 nm diameter decahedral nanoparticle with a monolayer coating of thiophenol. Spectral integration time is 2 seconds. The fluorescence-background has not been subtracted from the spectrum. The signal-to-noise-ratio is estimated to be ~16.

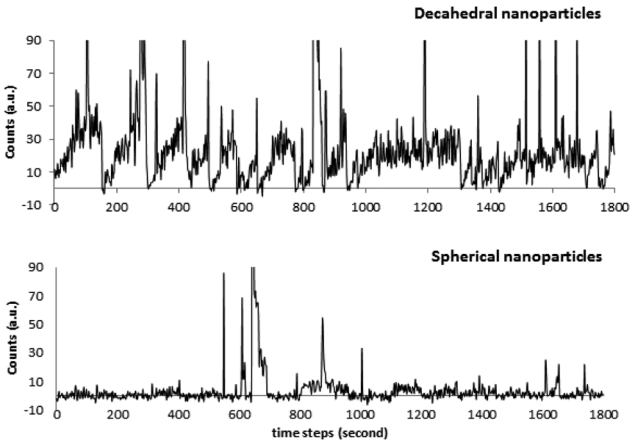

Fig. 4 Raman bursts for the C–C band at 1586 cm^{-1} from surface-adsorbed thiophenol on (a) a 36 nm decahedral silver nanoparticle and (b) a 40 nm spherical silver nanoparticle. Suspensions were made in Tris pH 7.4 buffer solution at the same concentration. Bursts are integrated over a 2 second interval. The number of counts measured for the maximum of the C–C symmetric peak is adjusted for background by subtracting the average readings from either side of the band feature.

There is a distinct difference between the two traces and the same data is presented as a histogram in Fig. 4 in order to compare the intensity of the peak maximum for the C–C band in thiophenol. For the decahedral nanoparticles over 75% (equivalent to 839/900) of the spectra recorded intensity above 10 counts for the C–C band. This compares to less than 7% (61/900) of the spectra for the spherical nanoparticles recording intensity for the C–C symmetric stretching band above 10 counts.

Fig. 3–6 demonstrates the ability of a single silver decahedral nanoparticle to enhance Raman scattering compared with a single spherical nanoparticle of similar dimensions. The shape of the decahedral nanoparticle leads to enhancement of the Raman signal to a level where it can be detected within an integration time of 2 seconds. These results are in agreement with Svedberg *et al.* where they showed that the Raman spectra from thiophenol on the surface of a spherical nanoparticle could not be detected from a single nanoparticle but could be detected when a nanoparticle pair, or a dimer, was formed.[11] It is believed that the infrequent positive SERS bursts for the spherical nanoparticles are a result of trapping more than one particle at a time and those particles being sufficiently close to form a dimer similar to the observations made by Svedberg *et al.* 2006.[11]

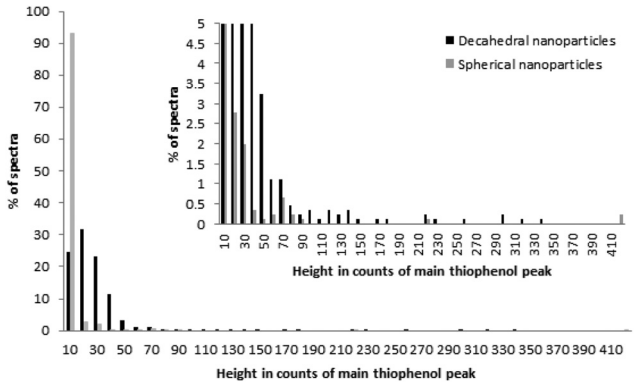

Fig. 5 The data presented in Fig. 2 plotted as a histogram in which the intensity of Raman-scattered light recorded at the maximum of the C–C band in thiophenol has been placed into bins of 10 counts. Inset – a magnified representation of the data with low percentages. The histogram compares the data taken with a 36 nm silver decahedral nanoparticle to that taken with a 40 nm silver spherical nanoparticle.

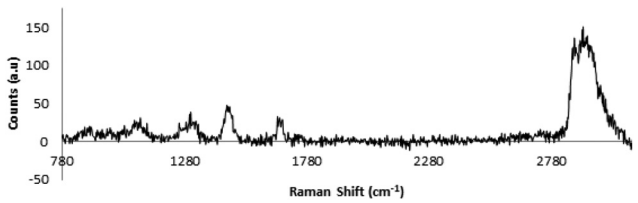

Fig. 6 A Raman spectrum recorded for 2 seconds from an optically-trapped GUV with a diameter of approximately 5 μm showing five clear lipid peaks at 1094, 1317, 1458, 1672 and 2935 cm^{-1}. A background signal has been subtracted.

Characterization of the lipid Raman spectra

The position and appearance of features in the Raman spectrum is known to vary according to composition and structural ordering of lipid molecules in a membrane, therefore the Raman spectrum for a giant unilamellar vesicle (GUV) made from the same lipid composition as the 50 nm vesicles was analyzed in order to characterize the measured bands originating from lipid molecules in the bilayer (see the Methods section for full details of the lipid composition). The spectrum shown in Fig. 6 was measured for an optically-trapped GUV with a diameter of approximately 5 μm. The acquisition time for the spectral measurement was 2 seconds. Five distinct lipid peaks were identified at 1094 cm^{-1} (a C–C skeletal stretching vibration), at 1317 cm^{-1} and 1458 cm^{-1} (a $-CH_2$ twist and bending vibration), at 1672 cm^{-1} (a *cis*-C=C stretching vibration) and at 2935 cm^{-1} (a superposition of CH_2 symmetric and asymmetric stretching vibrations).[21]

SERS enhancement from membrane encapsulated decahedral nanoparticles

In order to assess the ability of membrane-encapsulated nanoparticles to generate a SERS signal, a number of different samples were compared using the technique outlined above: (a) 50 nm-diameter liposomes with an aqueous core, (b) 40 nm spherical nanoparticles encapsulated in a 50 nm liposome, (c) 35–37 nm decahedral nanoparticles encapsulated in a 50 nm liposome, (d) 41 nm decahedral nanoparticles encapsulated in a 50 nm liposome, and (e) 43.5–44 nm decahedral nanoparticles encapsulated in a 50 nm liposome. The concentration of vesicles in suspension was kept low in order to reduce the probability of multiple vesicles falling into the trap at any one time and to ensure single vesicle trapping. The total number of vesicles present in a sample was estimated by multiplying the mole amount of lipid used in the sample preparation process by the estimated cross-sectional area of a lipid molecule (~0.82 nm^2 from ref. 2), divided by the combined surface area of inner and outer bilayer leaflets of a vesicle (*i.e.* $\sim 2 \times 4\pi a^2$, where a = 25 nm). We estimate 1 vesicle for every 9 μm^3 or an average separation of 3 μm between the 50 nm diameter vesicles.

Fig. 7 shows an example Raman spectrum for a single decahedral nanoparticle of 41 nm-diameter encapsulated in a liposome. The lipid peaks in the Raman spectrum in Fig. 7 are clearly visible and, in particular, the peaks at 1458 cm^{-1} and 2935 cm^{-1} (corresponding to the $-CH_2$ bending vibration and the superposition of the CH symmetric and asymmetric stretching vibrations of the methyl and methylene groups respectively) are in good agreement with Fig. 6. The presence of the lipid peaks confirm that the membrane remains intact during the experiment. For each of the seven samples listed above, 1800 × 1 s spectra were generated over a time period of 30 minute and Fig. 8 compares the measured Raman burst plots for each of these samples. Counts relate to the height of the most intense lipid peak at 2935 cm^{-1} (adjusted for background), see Fig. 6 and 7.

The data presented in the Raman burst plots (Fig. 8) has been used to generate the histograms shown in Fig. 9 for the percentage of spectra where the height of the lipid peak at 2935 cm^{-1} is within a certain range. For both the 50 nm diameter liposomes (Fig. 8a), without a nanoparticle, and the membrane-encapsulated spherical nanoparticles (Fig. 8b), 100% of the Raman spectra had a count number of 5 or lower for the lipid peak at 2935 cm^{-1} indicating the absence of any Raman signal above the background level, as expected. For the membrane-encapsulated decahedral nanoparticles of 36 nm-diameter (Fig. 8c), only 0.06% of the recorded spectra (equi-

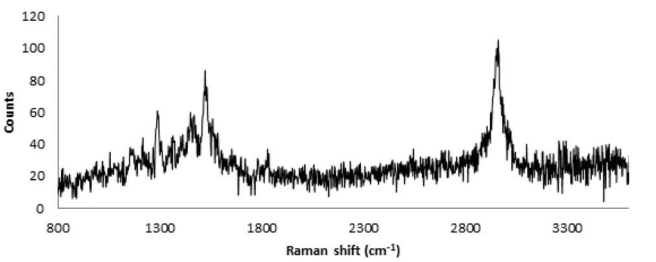

Fig. 7 A Raman spectrum recorded from an optically-trapped 50 nm lipid vesicle encapsulating a 41 nm diameter decahedral silver nanoparticle. The acquisition time was 1 second and a background signal has been subtracted. The signal-to-noise-ratio is estimated to be between 10 and 15.

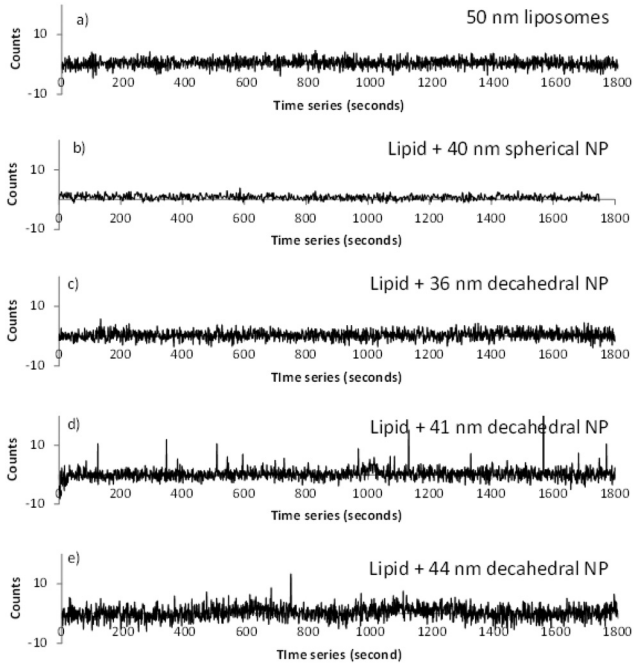

Fig. 8 Raman burst plots for the different liposome encapsulated nanoparticle samples: (a) 50 nm diameter liposomes with an aqueous core (control), (b) 40 nm spherical nanoparticles encapsulated in a 50 nm liposome, (c) 35–37 nm decahedral nanoparticles encapsulated in a 50 nm liposome, (d) 41 nm decahedral nanoparticles encapsulated in a 50 nm liposome, and (e) 43.5–44 nm decahedral nanoparticles encapsulated in a 50 nm liposome. The background adjusted height of the lipid peak at 2935 cm^{-1} is plotted for each of the 1 s spectra to show the Raman bursts where the nanoparticle has successfully enhanced Raman scattering from the lipid.

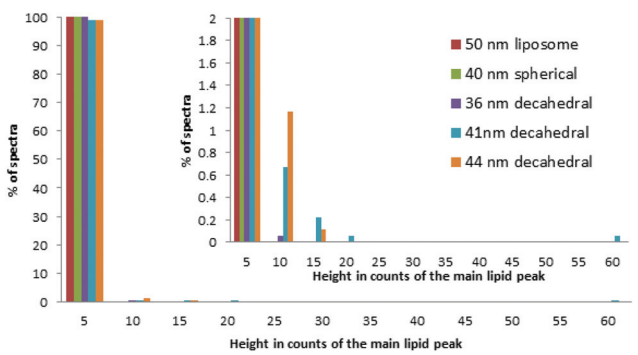

Fig. 9 The data presented in Fig. 6 plotted as a histogram in which the intensity of Raman-scattered light recorded at the maximum of the lipid peak at 2935 cm^{-1} has been placed into bins of 10 counts. Inset – a magnified representation of the data with low percentages.

valent to 1/1800) showed a Raman signal above 5 counts (the estimated background level) for the lipid peak at 2935 cm^{-1}. This compares to 1% (18/1800) of the recorded spectra for the membrane-encapsulated decahedral nanoparticles of 41 nm diameter (Fig. 8d) and 1.28% (23/1800) of the recorded spectra for the membrane-encapsulated decahedral nanoparticles of 44 nm-diameter (Fig. 8e).

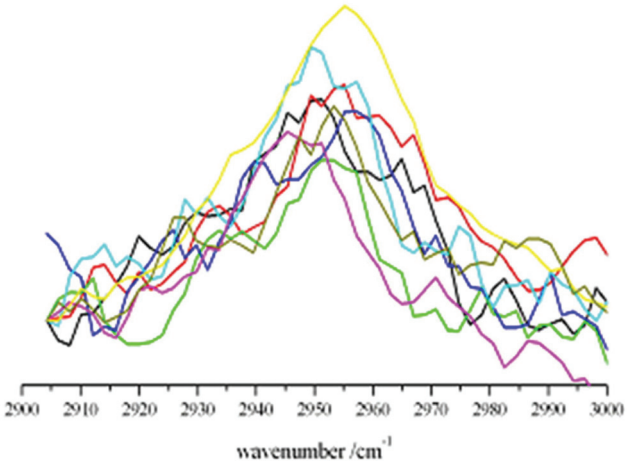

Fig. 10 The main lipid peak for 8 overlapping example spectra recorded from 41 nm diameter decahedral nanoparticles encapsulated in 50 nm lipid vesicles. Each plot representing a different single vesicle made from the same lipid composition highlighting the reproducibility of the results.

In Fig. 10 the main lipid peak is shown for 8 different vesicles each containing a liposome encapsulated 41 nm decahedral nanoparticle made from the same lipid composition. These overlapping spectra demonstrate the reproducibility of this technique.

Discussion

If two or more vesicles were optically trapped at any one time then a scattering 'hot spot' could occur at the contact point between the vesicles, this would be true for membrane-encapsulated spherical nanoparticles as well as membrane-encapsulated decahedral nanoparticles. The absence of any peaks or Raman bursts for the encapsulated spherical nanoparticles supports the argument that only single vesicles were held in the optical trap at any one time. In addition, if the number of vesicles in the trap were building up over time then the number of counts in Fig. 8, proportional to the number of Raman scattered photons, would also be expected to increase. As can be seen in Fig. 8, this is not the case and discrete peaks of high count number are observed on for the decahedral case suggesting a single vesicle optically trapped for a period of roughly 1–2 seconds.

The variation in the level of enhancement of Raman signals observed for the 3 different-sized decahedral nanoparticles is likely to be due to the proximity of the nanoparticle to the inner leaflet of the lipid bilayer. The SERS enhancement is known to fall off steeply with distance and, (assuming a 4.0 ± 0.5 nm thick lipid bilayer and vesicle outer diameter of 50 nm (ref. 2 and 18)) the gap of ~3 nm between the lipid bilayer and the nanoparticle for the 36 nm decahedra was too large to produce a SERS signal. The 41 nm and 44 nm decahedral nanoparticles showed a similar number of SERS bursts in the

measured Raman spectra (above the threshold of 5 counts). The 41 nm decahedral nanoparticles are predicted to have a gap of ~0.5 nm between the metal and inner leaflet of the lipid bilayer. These calculations assume a uniform diameter for the nanoparticle but, of course, the gap between a decahedral nanoparticle and the inner leaflet will vary; thus, the figures given reflect the predicted-minimum gap only. In theory, the membrane-encapsulated 44 nm decahedral nanoparticles should not fit through the 50 nm pores in the extruder, thus highlighting the range in particle diameters of the decahedral nanoparticle samples. The scanning electron microscope and TEM images reported by Pietrobon *et al.* show a range in diameters of the decahedral nanoparticles of ~±3 nm.[16] Lipid vesicles made *via* the extrusion method have been shown to vary by ±10 nm.[17]

Illuminating a metal nanoparticle with laser light would be expected to result in a temperature increase. Here, in particular, we need to consider any heating that might cause the lipid membrane to undergo a phase transition or, potentially, for it to be destroyed. Seol *et al.* modelled the temperature gradient surrounding a spherical 100 nm diameter gold particle trapped by a 1064 nm-wavelength laser beam and reported that the optical absorption of gold caused heating of 266 °C W^{-1} at the surface of the particle.[22] The rise in temperature is proportional to the laser beam power and the wavelength dependent absorption cross-section of the Rayleigh nanoparticle which is determined by the dielectric constant and volume of the particle.[22] We estimate heating of ~1.5 °C at the surface of our nanoparticles due to the optical trapping laser by assuming the dielectric constants of gold and silver are similar at 1064 nm and scaling for laser power and particle size, *i.e.* trapping a 40 nm diameter particle with 900 mW at a wavelength of 1070 nm. This calculation assumes that the heating due to a spherical nanoparticle will be the same as a decahedral nanoparticle, in practice the heating will depend on the shape of the nanoparticle (as shown by Ma *et al.*[23]) and is anticipated to be higher for the decahedral nanoparticle compared to the spherical. The Raman laser with a power of ~5 mW, operating at a wavelength of 488 nm, will also induce heating. Pietrobon *et al.* showed that the absorbance maximum for the decahedral nanoparticles occurred in the wavelength range of 450 nm to 470 nm depending on the particle size, with the 41 nm decahedral nanoparticles having an absorption cross-section at 488 nm approximately 600 times larger than at 1070 nm.[16] Scaling for power and absorption cross-section, we estimate that the Raman laser will heat the nanoparticle by a further ~5 °C. The presence of the lipid Raman spectra, as shown in Fig. 7 and 8, confirms that the lipid bilayer remains intact during the experiment.

It is interesting to consider if the stable trapping of 50 nm liposomes would be possible in the absence of a silver nanoparticle core. Gradient-force optical trapping relies on a difference in refractive index between a particle and the surrounding medium. Salamon *et al.*[24] measured the average refractive index of a lipid bilayer as 1.495, the aqueous phase interior (in the absence of silver nanoparticles) and the suspending solution for the liposomes has a refractive index of 1.360 (*i.e.* Tris buffer). The Rayleigh regime is defined as when the particle diameter $2a \leq 0.2\lambda$, where λ is the wavelength of the optical trapping laser beam. Here, a = 20 nm and λ = 1070 nm and the particles can be considered to be in the Rayleigh regime. In 1994 Svoboda *et al.*[25] studied the optical trapping of metallic Rayleigh particles and, using a similar approach to Ashkin *et al.* in 1986,[26] set out two criteria that must be met for the stable trapping of Rayleigh particles. Firstly, the gradient force must be greater than the scattering force and, secondly, the potential-energy minimum of the optical trap must significantly exceed thermal energies to achieve stable trapping, *i.e.* the time to pull an object into the trap must be considerably shorter than the time it would take the object to diffuse out of the trap due to Brownian motion. The 40 nm diameter silver nanoparticles were held in a stable optical trap for approximately 1–2 seconds before they escaped, which is comparable to the 5 second escape time observed by Svoboda *et al.*[25] when trapping 36 nm diameter gold nanoparticles with a similar laser beam power and wavelength. This time window was sufficient to detect ample Raman scattered photons and produce a clear spectrum.

Svoboda *et al.*[25] compared the trapping forces of a 36 nm-diameter spherical gold nanoparticle and a 38 nm diameter latex bead and showed, both experimentally and theoretically, the ratio of trapping forces equals the ratio of polarizabilities of the two particles. The gold particle could be trapped ~7 times more strongly than the latex particles. The average refractive index of a 50 nm liposome, accounting for the aqueous core, is calculated to be 1.386 (using the equations laid out in Matsuzaki *et al.*[27]). Taking the dielectric constant of silver at a wavelength of 1070 nm to be $\hat{\varepsilon} = -59.2 + 1.2i$,[28] we can determine how much stronger a 40 nm-diameter spherical silver nanoparticle will be optically trapped compared to a 50 nm diameter liposome. The polarizability, α, is given by,

$$\alpha = 3V\frac{\hat{\varepsilon} - \varepsilon_{\mathrm{m}}}{\hat{\varepsilon} + 2\varepsilon_{\mathrm{m}}} \quad (1)$$

where ε_{m} is the dielectric constant of the surrounding medium and V is the nanoparticle volume. The amplitude of an electromagnetic wave is known to penetrate a characteristic distance into a metallic medium; this distance is termed the skin depth, δ. When the skin depth is comparable to the radius of the trapped object, as is the case here, V is replaced by V' to account for the decrease in gradient force due to attenuation of the electric field, where,

$$V' = 4\pi\int_0^a r^2 \exp\left[\frac{r-a}{\delta}\right]\mathrm{d}r \quad (2)$$

The polarizability of a 40 nm diameter spherical silver nanoparticle is calculated to be 8.91×10^{-17} cm^3 as opposed to 2.50×10^{-18} cm^3 for a 50 nm diameter liposomes, giving a ratio of 35.7 and resulting in an estimate that a silver nanoparticle can be trapped ~36 times more strongly than a liposome for the same laser beam power. Therefore, the

encapsulated silver nanoparticle plays a critical role in increasing the polarizability and refractive index of the vesicle allowing it to be isolated and confined by an optical trap, as well as being essential for enhancing Raman scattering to a level where is can be detected. The calculations above for a spherical silver nanoparticle can be assumed to be representative of the decahedral nanoparticles where the laser wavelengths are off-resonance with the plasmon frequency.

Silver nanoparticles are inert but a citrate coating on the surface is expected to result in electrostatic interactions between the particle and the lipid bilayer. Specifically, these interactions will involve the choline (quaternary ammonium) head group on the lipid molecules and the negatively-charged citrate. There is good evidence in the literature that a citrate-coated nanoparticle will alter the tilt angle and perturb the fluidity of lipid molecules in the bilayer.[29] This electrostatic interaction does not entirely hinder the lateral diffusion and rotation of lipid molecules though. The *trans–gauche* isomerisation of hydrocarbon chains remains in the bilayer coating of the silver nanoparticle and we do not expect the lipid molecules to be arranged in a planar triangular lattice characteristic of a gel.

We have confirmed that there is no significant change in membrane fluidity by recording the excitation spectra of a fluorescent membrane probe, Di-8-ANEPPS (a styrylpyridinium dye). Di-8-ANEPPS has an excitation spectrum that exhibits a chromatic shift in response to changes in the dipole potential but has been shown to be insensitive to specific molecular interactions.[30,31] Di-8-ANEPPS is insensitive to small changes in lipid fluidity, as long as the bilayer membrane is maintained within the liquid-disordered phase. We appreciate that a small perturbation on the fluidity of lipid molecule is likely as a result of electrostatic interactions with the silver nanoparticle and the support substrate. Nevertheless, the fluorescent probe would be sensitive to the much more considerable change in the fluidity that takes place across the phase transition between liquid-disordered and gel structures of the membrane. We have compared the excitation spectra recorded at an emission wavelength of 580 nm for empty lipid vesicles and lipid vesicles containing silver nanoparticles and observe no chromatic shift confirming no significant change in membrane fluidity in accordance with Clarke.[30]

Conclusions

We have shown for the first time that by encapsulating silver decahedral nanoparticles in a lipid bilayer, the Raman-scattered light can be measured from an exceptionally small number of lipid molecules (~1.6×10^4 lipid molecules, assuming an outer leaflet radius of 25 nm, inner leaflet radius of 21 nm and a lipid area of 0.82 nm^2; see ref. 2). The encapsulated decahedral nanoparticle is playing two important roles, firstly, it increases the average refractive index and polarizability of the vesicles enabling a single vesicle to be isolated in an optical trap for a period of a few seconds and, secondly, the local field 'hot-spots' at the tips of the decahedral nanoparticle significantly enhance the Raman scattering to a level where it can be detected over a time interval of 1 s. The presence of single-encapsulated nanoparticles in individual vesicles is confirmed by TEM images and dynamic-light scattering data has shown that the lipid-coated nanoparticles remain monodisperse in suspension. The absence of Raman bursts in control experiments using spherical nanoparticles encapsulated in liposomes is evidence that the nanoparticles do not aggregate in the optical trap. In the longer term this approach will enable much more localized studies on the membrane surface than is currently possible with existing Raman techniques.

Comparing our work to that of other label-free approaches for measuring the Raman Spectra of lipid molecules,[3–5] we achieve a similar counts per s with 100 to 100 000 times less lipid molecules representing a significant increase in sensitivity. The signal-to-noise ratio of the spectra could be further increased by use of a higher power 488 nm Raman scattering laser. The ability to probe and investigate processes involving a significantly lower number of lipid molecules than has previously been possible will provide a highly-sensitive route for observing local changes in structure of the bilayer and the presence of membrane-bound proteins.

Acknowledgements

This work was funded in part by the Engineering and Physical Sciences Research Council of the UK (EPSRC), grant EP/J017566/1. AJW acknowledges financial support from the Royal Academy of Engineering (UK)/EPSRC *via* a personal research fellowship. We thank Prof. K. Faulds and Dr S. Mabbott, University of Strathclyde, for useful initial discussions. VK and NC acknowledge NSERC (Canada) financial support.

Notes and references

1 M. J. Hope, M. B. Bally, G. Webb and P. R. Cullis, *Biochim. Biophys. Acta*, 1985, **812**, 55.
2 J. F. Nagle and S. Tristram-Nagle, *Biochim. Biophys. Acta*, 2000, **1469**, 159.
3 L. Chongsoo and C. D. Bain, *Biochim. Biophys. Acta*, 2005, **1711**, 59.
4 J. M. Sanderson and A. D. Ward, *Chem. Commun.*, 2004, 1120.
5 D. P. Cherney, J. C. Conboy and J. M. Harris, *Anal. Chem.*, 2003, **75**, 6621.
6 S. A. Meyer, E. C. Le Ru and P. G. Etchegoin, *J. Phys. Chem.*, 2010, **17**, 5515.
7 S. Ip, C. M. MacLaughlin, N. Gunari and G. C. Walker, *Langmuir*, 2011, **27**, 7024.
8 D. Bhowmik, K. R. Mote, C. M. MacLaughlin, N. Biswas, B. Chandra, J. K. Basu, G. C. Walker, P. K. Madhu and S. Maiti, *ACS Nano*, 2015, **9**, 9070.

9 G. McNay, D. Eustane, W. E. Smith, K. Faulds and D. Graham, *Appl. Spectrosc.*, 2011, **65**, 825.
10 H. Xu, J. Aizpurua, M. Käll and P. Apell, *Phys. Rev. E: Stat., Nonlinear, Soft Matter Phys.*, 2000, **62**, 4318.
11 F. Svedberg, Z. Li, H. Xu and M. Käll, *Nano Lett.*, 2006, **6**, 2639.
12 A. Tao, P. Sinsermsuksakul and P. Yang, *Angew. Chem., Int. Ed.*, 2006, **45**, 4597.
13 S. D. Standridge, G. C. Schatz and J. T. Hupp, *J. Am. Chem. Soc.*, 2009, **131**, 8407.
14 D. V. Petrov, *J. Opt. A: Pure Appl. Opt.*, 2007, **9**, S139.
15 K. Ramser, W. Wenseleers, S. Dewilde, S. Van Doorslaer and L. Moens, *Spectroscopy*, 2008, **22**, 287.
16 B. Pietrobon and V. Kitaev, *Chem. Mater.*, 2008, **20**, 5186.
17 L. D. Mayer, M. J. Hope and P. R. Cullis, *Biochim. Biophys. Acta*, 1986, **858**, 161.
18 J. Wall, C. A. Golding, M. Van Veen and P. O'Shea, *Mol. Membr. Biol.*, 1995, **12**, 183.
19 S. M. Rigby-Singleton, M. C. Davies, H. Harris, P. O'Shea and S. Allen, *Langmuir*, 2006, **22**, 6273.
20 A. Moscho, O. Orwar, D. T. Chiu, B. P. Modia and R. N. Zare, *Proc. Natl. Acad. Sci. U. S. A.*, 1996, **93**, 11443.
21 Z. D. Schultz and I. W. Levin, *Annu. Rev. Anal. Chem.*, 2011, **4**, 343.
22 Y. Seol, A. E. Carpenter and T. T. Perkins, *Opt. Lett.*, 2006, **31**, 2429.
23 H. Ma, P. M. Bendix and L. B. Oddershede, *Nano Lett.*, 2012, **12**, 3954.
24 Z. Salamon and G. Tollin, *Biophys. J.*, 2001, **80**, 1557.
25 K. Svoboda and S. M. Block, *Opt. Lett.*, 1994, **19**, 930.
26 A. Ashkin, J. M. Dziedzic, J. E. Bjorkholm and S. Chu, *Opt. Lett.*, 1986, **11**, 288.
27 K. Matsuzaki, O. Murase, K. Sugishita, S. Yoneyama, K. Akada and M. Ueha, *Biochim. Biophys. Acta*, 2000, **1467**, 219.
28 S. Babar and J. H. Weaver, *Appl. Opt.*, 2015, **54**, 477.
29 Y. Li and N. Gu, *J. Phys. Chem. B*, 2010, **114**, 2749.
30 R. J. Clarke, *Biochim. Biophys. Acta*, 1997, **1327**, 269.
31 D. Robinson, N. A. Besley, P. O'Shea and J. D. Hirst, *J. Phys. Chem. B*, 2011, **115**(14), 4160–4167.